Original paper

Subsolidus behavior of niobian rutile from the Písek region, Czech Republic: a model for exsolution in W- and $Fe^{2+}>>Fe^{3+}$-rich phases

Petr ČERNÝ[1], Milan NOVÁK[2*], Ron CHAPMAN[1], Karen J. FERREIRA[1]

[1]*Department of Geological Sciences, University of Manitoba, Winnipeg, Mb, Canada, R3T 2N2*
[2]*Department of Geological Sciences, Masaryk University, Kotlářská 2, 611 37 Brno, Czech Republic; mnovak@sci.muni.cz*
[*]*Corresponding author*

Niobian rutile with substantial W content is associated with black tourmaline, beryl, zircon, xenotime-(Y), monazite-(Ce), "písekite", and possibly pseudorutile or pseudobrookite in two cogenetic, beryl-columbite-subtype, granitic pegmatites at Písek and Údraž, southern Bohemia, Czech Republic. Crystals, up to 3×1 cm in size, consist of relics of a primary, phase-homogeneous but oscillatorilly zoned niobian rutile phase and of exsolution intergrowths of depleted niobian rutile with granular titanian-tungstenian ixiolite. Primary niobian rutile has the monorutile structure and shows extensive substitution $(Fe, Mn, Mg)^{2+}_{+1} (Nb, Ta)^{5+}_{+2} Ti^{4+}_{-3}$ (up to 26.34 wt. % Nb_2O_5 and 8.60 wt. % Ta_2O_5; 26 to 37 mol. % columbite component), significant $(Fe, Mn, Mg)^{2+}_{+1} W^{6+}_{+1} Ti^{4+}_{-2}$ (up to 3.12 wt. % WO_3) and minor $(Fe, Sc)^{3+}_{+1} (Nb, Ta)^{5+}_{+1} Ti^{4+}_{-2}$ substitutions. The values of $Fe^{2+}/(Fe^{2+}+ Fe^{3+})$ are high and average at ~ 0.8. Oscillatory zoning is controlled by Nb, Ta and Fe; variations in W are independent and erratic. Depleted niobian rutile still contains 8 to (rarely) 32 mol. % ferrocolumbite component. Individual grains of the exsolved orthorhombic ixiolite are commonly heterogeneous in terms of the W content. They display highly variable degree of the substitution $Fe^{2+}_{+1} W^{6+}_{+3} Nb^{5+}_{-4}$ (up to 49.00 wt. % WO_3), moderate but widespread $(Ti, Zr, Hf)^{4+}_{+3} (Fe, Mn, Mg, Ca)^{2+}_{-1} (Nb, Ta)^{5+}_{-2}$ (up to 9.83 wt. % TiO_2, 1.94 wt. % ZrO_2), and subordinate $(Fe, Sc)^{3+}_{+3} (Fe, Mn, Mg, Ca)^{2+}_{-2} (Nb, Ta)^{5+}_{-1}$ (up to 1.51 wt. % Sc_2O_3). Exsolution reveals the preference of Sn^{4+} and Fe^{3+} for the rutile structure, whereas Fe^{2+}, Mn, Mg, Nb, Ta, Sc, Zr, Hf and W are concentrated in the ixiolite. The results confirm the extent of the W substitution in pegmatitic niobian rutile and its significance for the style of subsolidus breakdown, on par with the magnitude of effects exerted by $(Nb > Ta + Fe^{2+})$, $(Nb > Ta + Sc + Fe^{3+})$, $(Nb > Ta + Fe^{2+}/Fe^{3+}\sim1)$, or $(Fe/Nb > 0.5)$.

1. Introduction

Niobian rutile has been known since 150 years ago, mainly under its currently varietal name "ilmenorutile". However, it does not represent a distinct mineral species, as it is only a (Fe, Nb)-enriched but still Ti-dominant derivative of rutile. Moreover, niobian rutile is in most cases exsolved into a (Fe, Nb)-depleted rutile + titanian ferrocolumbite (or titanian ixiolite). Relics of the original homogeneous phase are scarce and largely only microscopic in size (e.g., Černý et al. 1964, 1999, 2000b). Reverse cases of niobian rutile exsolved from titanian columbite (which develops a highly ordered columbite structure AB_2O_6 on heating) or from titanian ixiolite (which orders on heating into the wodginite structure ABC_2O_8) also abound (Černý et al. 1998). The primary homogeneous orthorhombic phase compositionally represents the (Fe, Nb)-dominant part of the $TiO_2–Fe^{2+}Nb_2O_6$ system, in contrast to its Ti-dominant tetragonal counterpart, the niobian rutile.

Compositional variability in niobian rutile and in its exsolution products in granitic pegmatites is controlled mainly by the oxidation state of Fe and by substitution of heterovalent cations other than Fe^{2+}, Mn^{2+}, Nb and Ta. Different types of primary compositions and their decomposition products include (i) the most common case with dominant $(Fe^{2+}Nb_2) Ti_{-3}$ substitution (e.g., Věžná, western Moravia, with exsolved titanian ferrocolumbite; e.g., Černý et al. 2000b); (ii) the much less widespread substitution $[(Fe, Sc)^{3+}Nb] Ti_{-2}$ (Norwegian localities, with exsolved titanian $(Fe, Sc)^{3+}NbO_4$ phase; Černý et al. 2000a; Černý and Chapman 2001; cf. also Sahama 1978; Voloshin et al. 1991); (iii) the so far unique case of about equal concentrations of Fe^{2+} and Fe^{3+} (McGuire pegmatite, Colorado, with a complex exsolution sequence involving pseudorutile I and II, "ferropseudobrookite", titanian ferrocolumbite and ilmenite; Černý et al. 1999); (iv) excess of Fe^{2+} over and above the $(Fe^{2+}Nb_2) Ti_{-3}$ substitution, which leads to the exsolution of Nb, Ta-rich armalcolite–pseudobrookite and Nb-rich ilmenite (e.g., Uher et al. 1998); and (v) texturally evident exsolution of tungstenian columbite from a $(Fe^{2+}W^{6+})$-bearing niobian rutile (Okrusch et al. 2003; cf. also Černý et al. 2000b). Other varieties with more exotic components have also been described in the literature, but from non-pegmatitic environments: with Sb (Graham and Morris 1973; Ur-

ban et al. 1992; Smith and Perseil 1997), unexsolved W (Graham and Morris 1978; Urban et al. 1992; Rice et al. 1998), and V (Urban et al. 1992). However, most of these varieties of rutile were fine-grained to microscopic in size, the quantities of substituting elements were largely minor, and exsolution controlled by the exotic elements was not observed.

In 1992 we have started a reconnaissance study of niobian rutile from the Písek pegmatite district in southern Bohemia, Czech Republic, where this mineral was traditionally reported as restricted to a single pegmatite "U údražského obrázku" at Údraž (Čech et al. 1964, 1981). Field work of J. Cícha (Prácheň Museum, Písek) discovered, however, additional localities of niobian rutile, one of which is very similar to the above Údraž pegmatite: "Obrázek I" at Písek. Our exploratory work also indicated that niobian rutile and its exsolution product from the Písek district are significantly enriched in W, much over and above the values reported from this area by Novák and Černý (1998).

To date, "rutile-nigrine" from the Písek district was mentioned by Vrba (1893), chemically analyzed by Kovář (1895) who did not detect the presence of Nb, and later examined by Nováček (1936) who provided the first comprehensive description. Čech et al. (1964) examined the niobian rutile optically and by X-ray powder diffraction, and recognized an exsolution pattern of a columbite phase in rutile matrix. However, W was detected by emission spectrographic analysis only in traces (cf. also Černý et al. 1964).

Thus, we examined the Údraž and Písek samples in more detail, to document the widespread occurrence of W. We present here (i) the data on niobian rutile from the two pegmatites mentioned above, (ii) an insight into the composition of the oscillatorilly zoned, W-bearing primary niobian rutile, (iii) characteristics of the depleted rutile and W-rich exsolution products, and (iv) of an associated unidentified (Ti, Fe)-rich phase, possibly related to pseudorutile or pseudobrookite.

2. The parental pegmatites and samples examined

The LCT-family pegmatites of the Písek region that yielded the examined niobian rutile are mutually very similar, and also bear resemblance to the Věžná I pegmatite in western Moravia (which is somewhat more evolved and modified by reaction with its host serpentinite). All three dikes belong to the beryl–columbite subtype of the rare-element (Li) subclass (cf. Černý and Ercit 2005; Novák 2005 for classifications).

The pegmatite at Údraž is poorly exposed today. Old reports suggest it consists of a medium-grained tourma-

line-bearing granitic zone, probably predominant over other, more centrally located units, such as a graphic feldspar + quartz zone. A feldspar-rich assemblage underlies a sizeable quartz core, with rose quartz dominant over white. Albite-rich unit is widespread, and most accessory minerals including niobian rutile are typically associated with albite. Niobian rutile is associated with columnar black tourmaline, brown monazite-(Ce), greenish-grey xenotime-(Y), and "písekite". Muscovite and greenish beryl are abundant, apatite and zircon much less so (Čech et al. 1981).

Seven samples of niobian rutile were examined from this pegmatite: ST-UDA, ST-UDB (J. Staněk), MMC-2, MMC-3 (collected by MN), and N34, N45 and N46 (Moravian Museum Brno).

The Obrázek I pegmatite at Písek shows blocky K-feldspar and albite unit overlain by a sizeable quartz core, which contains small vugs lined with crystals of smoky quartz. Besides rock-forming K-feldspar, albite and quartz, accessory beryl, black tourmaline (schorl to foitite), monazite-(Ce) and xenotime-(Y) are prominent. "Písekite" is not uncommon, whereas ilmenite, a member of the columbite group and several sulphides are minor. Hydrothermal alteration products include abundant bertrandite, apatite, albite and muscovite (Čech et al. 1981).

Four samples of niobian rutile were examined from the Obrázek I pegmatite: MMC-4, MMC-5 (collected by MN), ST3 (J. Staněk), and H14A (Moravian Museum Brno).

3. Experimental

Electron microprobe analyses were performed in the wavelength-dispersion mode on a Cameca SX-50 instrument at the Department of Geological Sciences, University of Manitoba, in part by MN but largely by RC. The analytical conditions of the oxide minerals and normalization of atomic contents were the same as for the niobian rutile from Věžná (Černý et al. 2000b): A beam diameter of 1 to 2 μm, accelerating potential of 15 kV, a sample current of 20 mA and a counting time of 20 s were used for Ti, Nb, Ta, Fe and Mn, and 40 mA and 50 s for W, Sb, Bi, As, Sc, Ca, Pb, Y, U, Zr and Hf. The following standards were used: manganotantalite (Ta$M\alpha$), MnNb$_2$O$_6$ (Mn$K\alpha$, Nb$L\alpha$). FeNb$_2$O$_6$ (Fe$K\alpha$), CaNb$_2$O$_6$ (Ca$K\alpha$), SnO$_2$ (Sn$L\alpha$), rutile (Ti$K\alpha$), BiTaO$_4$ (Bi$M\alpha$), mimetite (Pb$M\alpha$, As$L\alpha$), stibiotantalite (Sb$L\alpha$), NaScSi$_2$O$_6$ (Sc$K\alpha$), UO$_2$ (U$M\alpha$), YAG (Y$L\alpha$), ZrO$_2$ (Zr$L\alpha$), metallic Hf (Hf$K\alpha$) and metallic W (W$M\alpha$). Data were reduced using the PAP routine (Pouchou and Pichoir 1984, 1985). In some cases, the Zr and Hf contents were verified under conditions used by Černý et al. (2007). Ercit et al. (1992) provided

justification of the method of the ferric iron estimation. The same charge-balancing method resulting in calculated Fe^{3+}was used for normalization of the potential pseudo-

brookite. The niobian rutile and the exsolved phase were both normalized to 4 cations (atoms per 4 formula units) to facilitate mutual comparison of atomic contents.
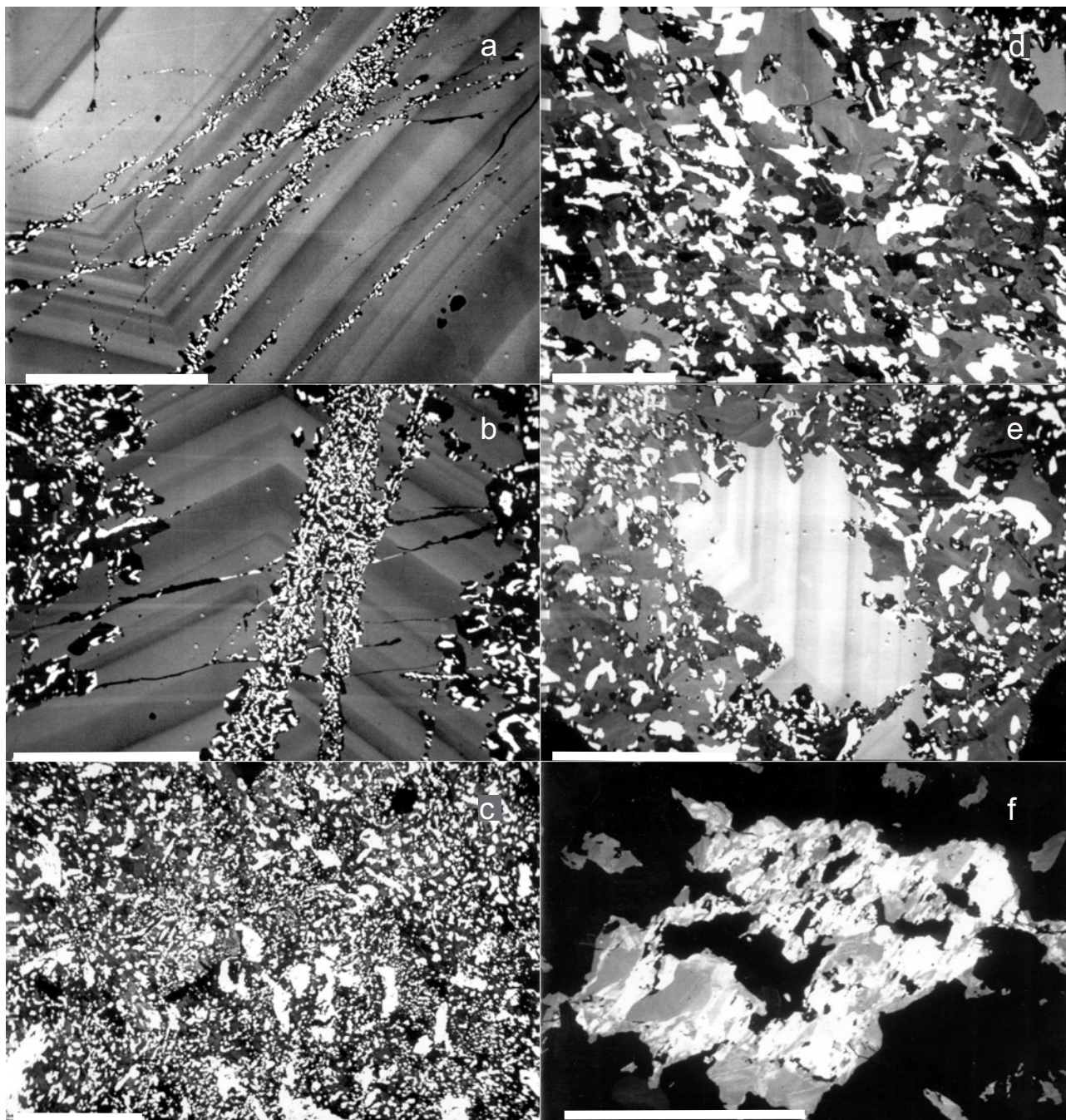

Fig. 1 BSE images of exsolution patterns in the Údraž niobian rutile: **a** – thin streaks of fine-grained ixiolite phase (white) in depleted rutile (black) across the oscillatory zoning of the primary niobian rutile; scale bar 500 μm; **b** – same as a, with coarser grain size of the ixiolite phase (white) but nearly uniform in each of the exsolved patches; scale bar 500 μm; **c** – random distribution of largely fine (~ 5 to 20 μm) up to coarser (#80 μm) grains of ixiolite (white) in heterogeneous matrix of depleted niobian rutile (grey to black); scale bar 200 μm; **d** – coarse-grained exsolution of ixiolite (white; up to 150 μm) in a heterogeneous matrix of depleted niobian rutile (grey to black); note the high concentration of exsolved ixiolite in the most depleted (i.e. the darkest) patches of niobian rutile; scale bar 200 μm; **e** – relic of primary, oscillatorilly zoned niobian rutile in a coarse intergrowth of depleted rutile (variable gray) and ixiolite (white; up to 300 μm), scale bar 500 μm; **f** – compositional heterogeneity of a large exsolution grain of ixiolite in depleted niobian rutile (black); the WO$_3$ content of the ixiolite grain varies from 3.62 wt. % in the dark-gray parts to 38.90 wt. % in the white parts; scale bar 100 μm.

4. General characteristics of niobian rutile from the Písek district

At both localities, columnar to stubby, steel-gray to black crystals of niobian rutile are associated dominantly with black tourmaline (schorl to foitite) in an albite matrix, with minor but persistent zircon, xenotime-(Y), monazite-(Ce) and probable brabantite. The crystals of niobian rutile are subhedral, pseudohexagonal, and attain 1×3 cm in size (cf. Nováček 1936 for details of morphology). Optical examination in reflected light and X-ray powder diffraction (XRD) (Čech et al. 1964; Černý et al. 1964), back-scattered electron images (BSE), and electron-microprobe analyses (EMPA) show that most of the niobian rutile is exsolved into a matrix of (Fe, Mn, Nb, Ta, W)-depleted rutile which hosts microgranules of an ixiolite phase.

Analysis of the two sets of data collected on samples from the two localities reveal a virtual identity of the textural, phase- and compositional properties of niobian rutile from both pegmatites. This is not particularly surprising, as both pegmatites belong to one and the same pegmatite group related to a common plutonic source (Čech et al. 1981), and they also show very similar assemblages of accessory rare-element minerals, strongly suggesting an analogous degree of geochemical evolution and regime of consolidation. Thus the results obtained on samples from both localities are pooled here and treated collectively; in some of the figures below, graphic separation of data from individual localities documents the near-perfect overlap of the two sets of data.

5. Primary niobian rutile

Primary phase-homogeneous niobian rutile yields XRD powder patterns of the monorutile structure. Diffractions indicative of birutile or trirutile superstructures were not observed. However, the primary crystals are almost invariably oscilatorilly zoned. The few cases which suggest compositional homogeneity consist of very small relics surrounded by aggregates of exsolved phases, and could represent grains accidentally cut (sub)parallel to zoning. In any case, the oscillatory zoning is at least a greatly predominant feature of the primary niobian rutile (Fig. 1 a–b, e).

Variations in Nb and Ta, individually as well as collectively, control the gross oscillatory patterns and are inverse to Ti (Fig. 2). In contrast, variations in W are erratic. On a very local scale, W seems to follow Ta and Nb or to counterbalance them (Fig. 2, N45B), but it mostly shows a relatively smooth increase with progress of crystallization (Fig. 2, N45A) or random patterns. Distribution of Fe and Mn follows primarily those of Nb
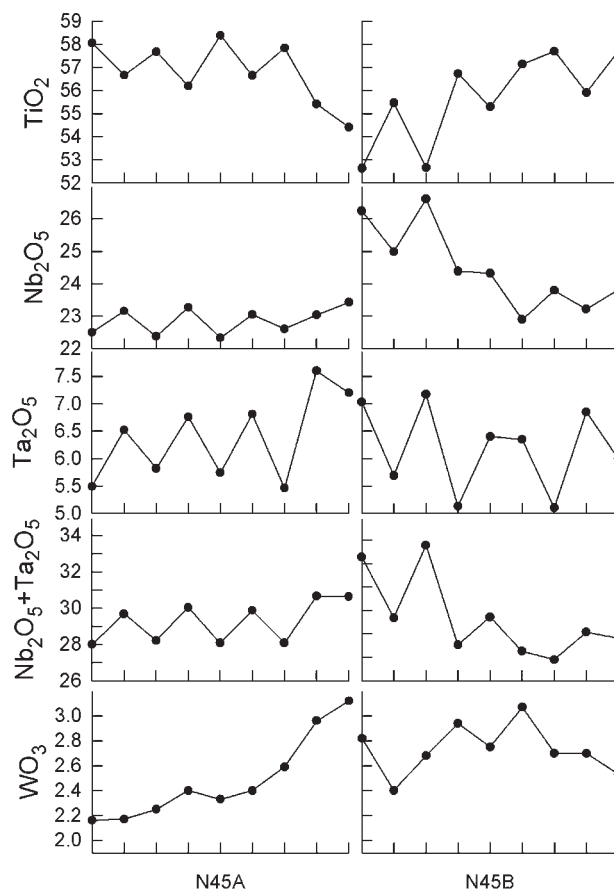

Fig. 2 Profiles across the oscillatory zoning of two crystals of primary niobian rutile, documenting the maxima and minima of each oscillation cycle. Horizontal scale arbitrarily schematized; growth direction to the right. The actual overall length of the sections is 1240 and 900 μm for A and B, respectively. Note the sympathetic variation in Ta_2O_5 and Nb_2O_5, reverse from that in TiO_2, and the largely independent behavior of WO_3 (wt. %).

and Ta, but their oscillations are somewhat moderated by the Fe and Mn that compensate for the independently variable W.

In detail, the individual oscillation cycles commonly reveal a regular pattern: in the direction of crystal growth, a narrow zone of low-level Nb and Ta (dark grey) is followed by a broader zone of slightly increased substitution (medium grey) and an even broader zone with high concentration of these elements (Fig. 1 a–b, e). Figure 3 shows a quantitative documentation of this stepped-up gradation.

Conspicuous as the oscillatory zoning is in the BSE images, the actual compositional variations are modest, ranging from 26 to 37 mol. % of the ferrocolumbite component (Fe >> Mn)(Nb > Ta)$_2$O$_6$ (Fig. 4a, 5a).

The proportion of the Fe^{3+}(Nb > Ta)O$_4$ component, so far unknown as an independent mineral species but recognized, in its Ti- and Sc-enriched form, as an exsolution product in niobian rutile from Norway (Černý et
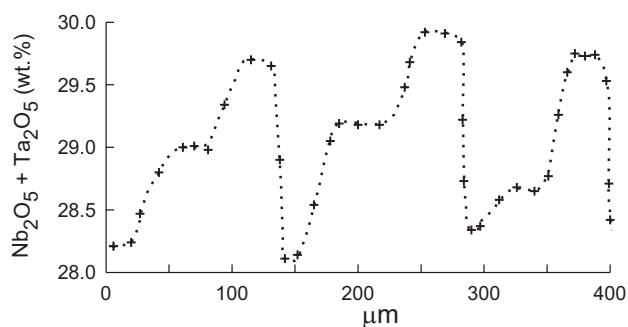
Fig. 3 Detailed section across a typical oscillatory zoning pattern observed in numerous crystals of primary niobian rutile, exemplified by the variation in the combined (and mutually sympathetic) $Nb_2O_5 + Ta_2O_5$ contents (wt. %). Fluctuations of the W content are independent of this pattern. Slight sideways shifts were introduced into the analyzed linear section in segments with very tight spacing of the analyzed spots. Growth direction to the right.

al. 2000a; Černý and Chapman 2001), and in zoned ferberite to "wolframoixiolite" at Dolní Bory (Novák et al. 2007), is negligible (Tab. 1, Figs 4a, 5a). The W content attains a modest maximum of 3.12 wt. % oxide, but it rarely drops below the 2 wt. % level. The $Mn/(Mn + Fe)$ (atomic) ratios are tightly clustered around 0.01, whereas the $Ta/(Ta + Nb)$ (atomic) data are slightly more variable between 0.11 and 0.17 (Figs 4b, 5b). The distribution of Ti approaches the Gaussian curve (Fig. 6a). The content of Zr is rather low (largely <0.1 wt. % oxide), as are the concentrations of Sn, Mn, Fe^{3+} and particularly Mg (Fig. 7a–b). Hafnium is close to detection limit of the analytical conditions employed. Traces of Ca, Zn, Pb, Sb, Bi, As, Y, U and Th are locally present (Tab. 1).

6. Depleted niobian rutile and exsolved titanian-tungstenian ixiolite

Powder XRD examination of the exsolution products shows the rutile matrix to possess the monorutile structure. Camera-recorded data (Čech et al. 1964; Černý et al. 1964) and our recent results from a powder diffractometer revealed only a few diffractions which indicate the presence of an orthorhombic columbite-type phase. However, diffractions which would unambiguously identify ordered columbite structure (low as their intensities would be) were not observed. In view of the noticeable contents of Ti, Zr, Sn, Sc and the highly variable but commonly substantial W content, a disordered structure is presumed more probable for the exsolved phase. Consequently, it is termed (titanian–tungstenian) ixiolite in the following text.

The exsolved ixiolite shows moderate but distinct variation in grain size. Examination of niobian rutile from other localities has shown significant variation in the chemical composition of exsolution products, and of

Tab. 1 Representative chemical compositions of primary oscillatorilly zoned niobian rutile (see Figs 1a–b, e, 2 and 3). All samples from Údraž, except H14 from Písek. Atomic contents based on 8 oxygen atoms and 4 cations.

Sample wt. %	45123	45B-6	45B-1	46A30	46A33	H14A2
WO_3	3.12	3.07	2.82	2.36	2.18	1.87
Nb_2O_5	23.43	22.90	26.24	23.81	24.83	25.65
Ta_2O_5	7.20	6.35	7.03	5.83	6.99	7.49
TiO_2	54.41	57.14	52.63	57.20	54.72	53.22
ZrO_2	0.10	0.39	0.05	0.12	0.04	0.03
SnO_2	0.33	0.27	0.34	0.33	0.38	0.44
ThO_2	0.02	0.03	0.00	0.00	0.12	0.00
UO_2	0.00	0.01	0.00	0.01	0.00	0.00
Sc_2O_3	0.15	0.15	0.10	0.15	0.20	0.19
Fe_2O_3	1.75	1.63	1.60	2.22	1.97	2.69
As_2O_3	0.01	0.00	0.02	0.00	0.05	0.03
Y_2O_3	0.00	0.02	0.04	0.00	0.00	0.02
Sb_2O_3	0.02	0.00	0.01	0.01	0.02	0.00
Bi_2O_3	0.00	0.03	0.00	0.00	0.00	0.08
MgO	0.02	0.02	0.03	0.03	0.02	0.01
CaO	0.00	0.00	0.00	0.00	0.01	0.00
MnO	0.02	0.10	0.07	0.05	0.06	0.15
FeO	7.54	7.21	8.19	6.93	7.36	7.21
ZnO	0.00	0.00	0.00	0.00	0.03	0.00
PbO	0.01	0.00	0.00	0.00	0.05	0.04
Total	98.13	99.32	99.17	99.05	99.03	99.12
W^{6+}	0.052	0.050	0.047	0.038	0.036	0.031
Nb^{5+}	0.680	0.650	0.759	0.674	0.713	0.739
Ta^{5+}	0.126	0.108	0.122	0.099	0.121	0.130
Ti^{4+}	2.628	2.699	2.532	2.694	2.612	2.551
Zr^{4+}	0.003	0.012	0.002	0.004	0.001	0.001
Sn^{4+}	0.008	0.007	0.009	0.008	0.010	0.011
Th^{4+}	0.000	0.000	0.000	0.000	0.002	0.000
U^{4+}	0.000	0.000	0.000	0.000	0.000	0.000
Sc^{3+}	0.008	0.008	0.006	0.008	0.011	0.011
Fe^{3+}	0.084	0.077	0.077	0.105	0.094	0.129
As^{3+}	0.000	0.000	0.001	0.000	0.002	0.001
Y^{3+}	0.000	0.001	0.001	0.000	0.000	0.001
Sb^{3+}	0.001	0.000	0.000	0.000	0.001	0.000
Bi^{3+}	0.000	0.000	0.000	0.000	0.000	0.001
Mg^{2+}	0.002	0.002	0.003	0.003	0.002	0.001
Ca^{2+}	0.000	0.000	0.000	0.000	0.001	0.000
Mn^{2+}	0.001	0.005	0.004	0.003	0.003	0.008
Fe^{2+}	0.405	0.379	0.438	0.363	0.391	0.384
Zn^{2+}	0.000	0.000	0.000	0.000	0.001	0.000
Pb^{2+}	0.000	0.000	0.000	0.000	0.001	0.001

the adjacent rutile matrix, with grain size (Černý et al. 2000a, b). Thus the population of exsolution products analyzed in the present study was subdivided into two size groups, suggested by the approximate frequency of their dimensions (fine-grained from a safely analyzable minimum of ~10 to ~50 μm, coarse-grained from ~50 to a maximum of ~300 μm), to detect any potential com-
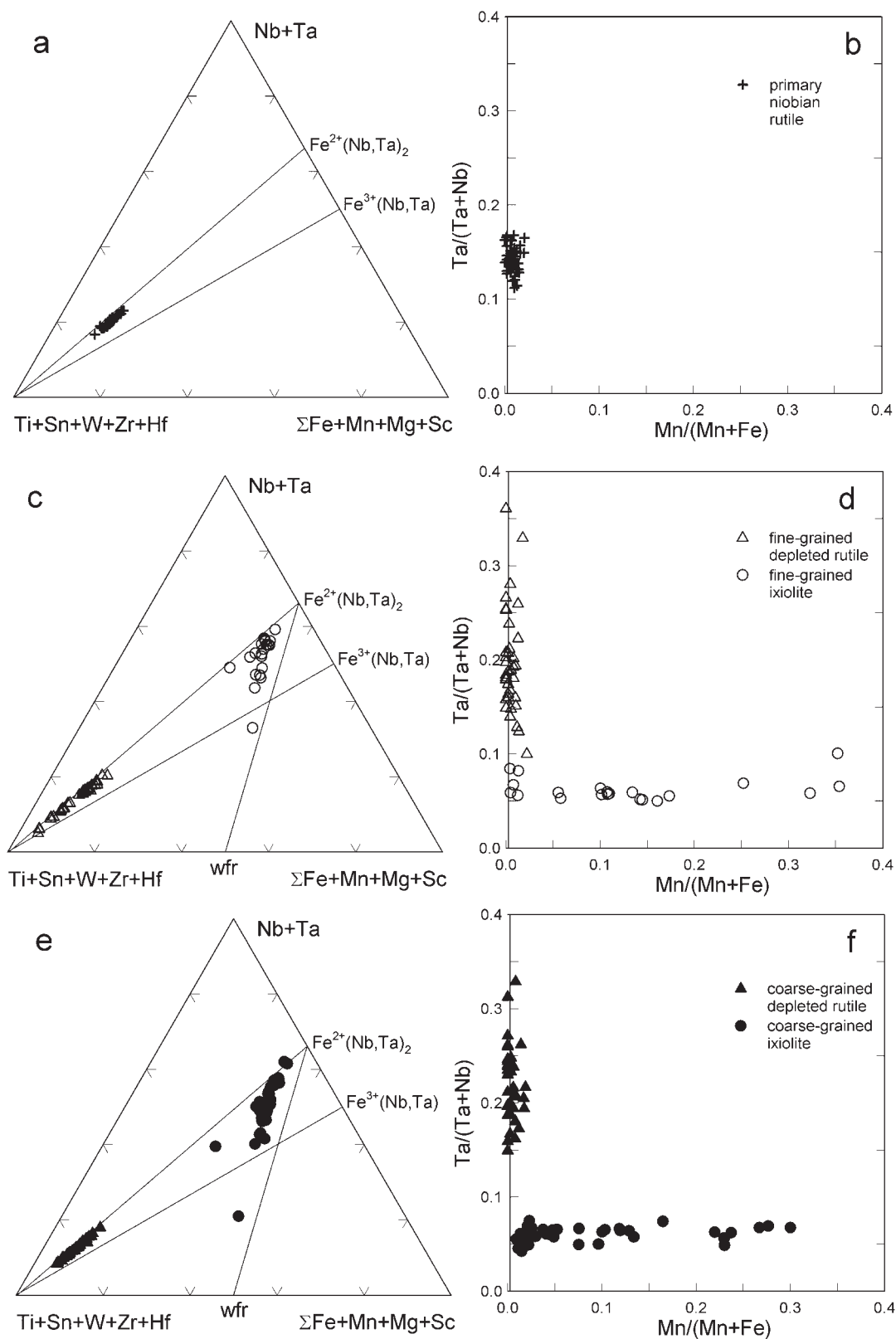
Fig. 4 Compositions of the niobian rutile and ixiolite from Údraž in the ternary diagram (Nb + Ta) – (Ti + Sn + W + Zr + Hf) – (Fe$_{tot}$ + Mn + Mg + Sc) (**a, c, e**) and in the columbite quadrilateral (**b, d, f**) (all atomic). In **a–c**, note the alignment of the niobian rutile along the Ti (rutile) – Fe^{2+}(Nb, Ta)$_2$ (columbite) join, and the trend of ixiolite parallel to the Fe^{2+}(Nb, Ta)$_2$ (columbite) – wfr (wolframite) join. In **d** and **f**, note the relative enrichment of the depleted niobian rutile in Ta, and of the ixiolite phase in Mn.
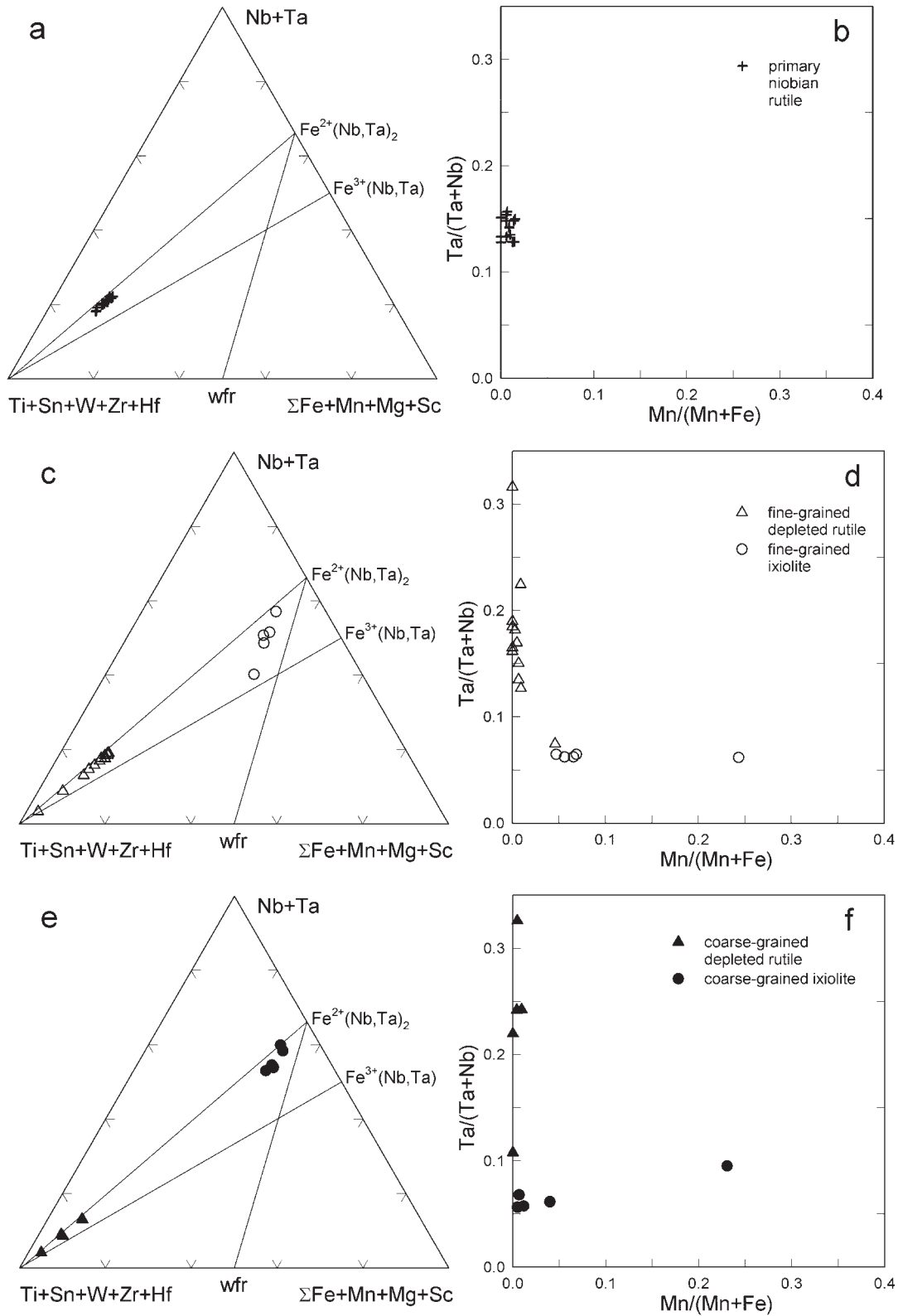
Fig. 5 Compositions of the niobian rutile and ixiolite from Písek in the ternary diagram (Nb + Ta) – (Ti + Sn + W + Zr + Hf) – (Fe$_{tot}$ + Mn + Mg + Sc) (**a, c, e**) and in the columbite quadrilateral (**b, d, f**) (all atomic). In **a–c**, note the alignment of the niobian rutile along the Ti (rutile) – Fe^{2+}(Nb, Ta)$_2$ (columbite) join, and the trend of ixiolite parallel to the Fe^{2+}(Nb, Ta)$_2$ (columbite) – wfr (wolframite) join. In **d** and **f**, note the relative enrichment of the depleted niobian rutile in Ta, and of the ixiolite phase in Mn. Note the virtual identity of the data distribution with those in Fig. 4.

Tab. 2 Representative chemical compositions of fine-grained and coarse-grained depleted niobian rutile which hosts an exsolved ixiolite phase (see Figs 1–3, Tab. 3). All samples from Údraž. Atomic contents based on 8 oxygen atoms and 4 cations.

Sample wt. %	fine-grained			coarse-grained		
	N34A4	N3413	N46A9	46A14	UDA3	45113
WO_3	2.13	0.92	0.32	1.01	0.43	0.20
Nb_2O_5	24.21	20.37	6.57	16.92	9.81	9.71
Ta_2O_5	7.04	6.47	5.36	6.21	5.14	5.99
TiO_2	55.05	62.45	84.25	67.10	79.51	78.51
ZrO_2	0.24	0.00	0.00	0.00	0.00	0.00
SnO_2	0.48	0.41	0.22	0.57	0.43	0.20
ThO_2	0.01	0.00	0.00	0.06	0.00	0.00
UO_2	0.00	0.05	0.00	0.00	0.11	0.00
Sc_2O_3	0.11	0.06	0.00	0.07	0.02	0.00
Fe_2O_3	2.88	2.21	1.97	3.49	1.54	1.58
As_2O_3	0.02	0.01	0.02	0.05	0.01	0.02
Y_2O_3	0.01	0.00	0.02	0.06	0.01	0.01
Sb_2O_3	0.00	0.00	0.00	0.05	0.00	0.00
Bi_2O_3	0.13	0.02	0.05	0.00	0.16	0.12
MgO	0.01	0.00	0.00	0.01	0.00	0.00
CaO	0.00	0.00	0.01	0.01	0.00	0.00
MnO	0.00	0.07	0.06	0.05	0.00	0.01
FeO	6.95	5.74	1.75	4.16	2.89	2.90
ZnO	0.00	0.00	0.02	0.00	0.00	0.00
PbO	0.00	0.00	0.00	0.00	0.00	0.04
Total	99.27	98.78	100.62	99.82	100.06	99.29
W^{6+}	0.035	0.015	0.005	0.016	0.006	0.003
Nb^{5+}	0.692	0.567	0.167	0.459	0.255	0.255
Ta^{5+}	0.121	0.108	0.082	0.101	0.080	0.095
Ti^{4+}	2.618	2.893	3.569	3.030	3.438	3.429
Zr^{4+}	0.007	0.000	0.000	0.000	0.000	0.000
Sn^{4+}	0.012	0.010	0.005	0.014	0.010	0.005
Th^{4+}	0.000	0.000	0.000	0.001	0.000	0.000
U^{4+}	0.000	0.001	0.000	0.000	0.001	0.000
Sc^{3+}	0.006	0.003	0.000	0.004	0.001	0.000
Fe^{3+}	0.137	0.103	0.083	0.158	0.066	0.069
As^{3+}	0.001	0.000	0.001	0.002	0.000	0.001
Y^{3+}	0.000	0.000	0.001	0.002	0.000	0.000
Sb^{3+}	0.000	0.000	0.000	0.001	0.000	0.000
Bi^{3+}	0.002	0.000	0.001	0.000	0.002	0.002
Mg^{2+}	0.001	0.000	0.000	0.001	0.000	0.000
Ca^{2+}	0.000	0.000	0.001	0.001	0.000	0.000
Mn^{2+}	0.000	0.004	0.003	0.003	0.000	0.000
Fe^{2+}	0.367	0.296	0.082	0.209	0.139	0.141
Zn^{2+}	0.000	0.000	0.001	0.000	0.000	0.000
Pb^{2+}	0.000	0.000	0.000	0.000	0.000	0.001

Tab. 3 Representative chemical compositions of the fine-grained and coarse-grained ixiolite phase exsolved from niobian rutile (see. Fig. 1, Tab. 2). All samples from Údraž. Atomic contents based on 8 oxygen atoms and 4 cations.

Sample wt. %	fine-grained			coarse-grained		
	N3419	UDB3	46A35	N34A1	45B30	45B27
WO_3	15.88	10.93	5.69	49.00	26.60	19.83
Nb_2O_5	50.82	56.66	61.20	19.13	42.51	48.48
Ta_2O_5	5.75	5.27	6.06	2.55	3.64	4.25
TiO_2	5.33	5.82	6.00	4.75	4.30	5.18
ZrO_2	0.62	0.84	0.89	1.34	1.16	1.14
SnO_2	0.26	0.34	0.25	0.40	0.08	0.19
HfO_2	0.09	0.18	0.10	0.07	0.02	0.08
ThO_2	0.00	0.00	0.06	0.03	0.02	0.00
UO_2	0.05	0.01	0.00	0.11	0.00	0.12
Sc_2O_3	1.18	1.01	0.60	1.33	0.80	0.78
Fe_2O_3	0.67	0.00	0.00	0.53	0.92	0.00
As_2O_3	0.00	0.00	0.03	0.00	0.00	0.00
Y_2O_3	0.00	0.08	0.03	0.00	0.05	0.01
Sb_2O_3	0.00	0.01	0.00	0.00	0.02	0.00
Bi_2O_3	0.01	0.00	0.00	0.06	0.00	0.00
MgO	0.07	0.06	0.04	0.06	0.13	0.13
CaO	0.00	0.01	0.00	0.02	0.00	0.01
MnO	1.90	1.07	0.23	3.28	4.56	1.82
FeO	16.62	17.49	18.35	16.37	14.62	17.28
PbO	0.00	0.00	0.00	0.03	0.00	0.00
Total	99.25	99.78	99.53	99.06	99.43	99.30
W^{6+}	0.328	0.220	0.113	1.138	0.567	0.413
Nb^{5+}	1.829	1.988	2.122	0.775	1.580	1.763
Ta^{5+}	0.124	0.111	0.126	0.062	0.081	0.093
Ti^{4+}	0.319	0.340	0.346	0.320	0.266	0.313
Zr^{4+}	0.024	0.032	0.033	0.059	0.047	0.045
Sn^{4+}	0.008	0.011	0.008	0.014	0.003	0.006
Hf^{4+}	0.002	0.004	0.002	0.002	0.000	0.002
Th^{4+}	0.000	0.000	0.001	0.001	0.000	0.000
U^{4+}	0.001	0.000	0.000	0.002	0.000	0.002
Sc^{3+}	0.082	0.068	0.040	0.104	0.057	0.055
Fe^{3+}	0.040	0.000	0.000	0.035	0.057	0.000
As^{3+}	0.000	0.000	0.001	0.000	0.000	0.000
Y^{3+}	0.000	0.003	0.001	0.000	0.002	0.000
Sb^{3+}	0.000	0.000	0.000	0.000	0.001	0.000
Bi^{3+}	0.000	0.000	0.000	0.001	0.000	0.000
Mg^{2+}	0.008	0.007	0.005	0.008	0.016	0.016
Ca^{2+}	0.000	0.001	0.000	0.002	0.000	0.001
Mn^{2+}	0.128	0.070	0.015	0.249	0.318	0.124
Fe^{2+}	1.106	1.135	1.177	1.227	1.006	1.162
Pb^{2+}	0.000	0.000	0.000	0.001	0.000	0.000

positional differences. The adjacent matrices of depleted rutile were subdivided accordingly.

The rutile matrix is locally near-homogeneous at a scale of ~1 mm (Fig. 1b), but in most cases heterogeneous (Fig. 1 c–f) and indicative of uneven degree of exsolution. This is reflected in a broad range of the un-exsolved columbite component (5 to 32 mol. %, Figs 4c, e, 5c, e). Figures 4d, f and 5d, f show that the Mn/(Mn + Fe) values remain in the same bracket as those of the primary homogeneous rutile phase, but the Ta/(Ta +
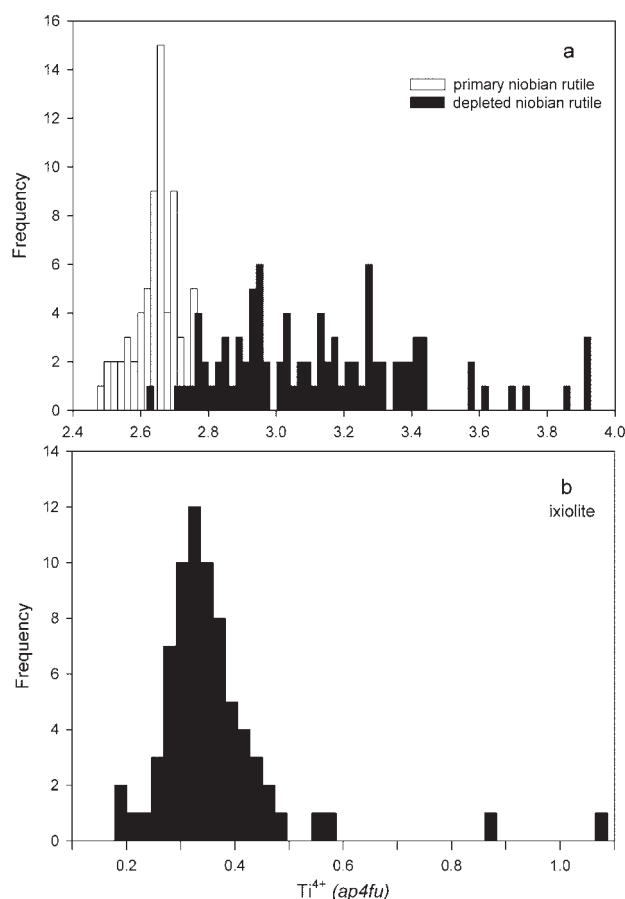
Fig. 6 Histograms of Ti^{4+} contents in the primary niobian rutile and depleted niobian rutile **(a)**, and in the exsolved ixiolite **(b)**. All data in atoms per 4 formula units. Note the tight clustering of the primary niobian rutile and ixiolite, but the relatively broad dispersion of the depleted niobian rutile data.

Nb) ratio is highly disturbed (see Tab. 2). Oscillatory zoning of the primary niobian rutile was obliterated during the exsolution and, probably, fine recrystallization. The depleted rutile matrix is impoverished in Nb, Ta, Fe (particularly Fe^{2+} relative to Fe^{3+}), Mn, W, Zr and Sc, and enriched in Ti, relative to the primary homogeneous niobian rutile (Figs 4c, e and 5c, e vs. a, Fig. 6a, Fig. 7c; Tables 1 and 2).

The exsolved ixiolite phase shows a broad range of W content, which extends mainly from ~5 to ~40 mol. % of the wolframite component (Fe, Mn)WO_4 (wfr in Figs 4 and 5). Individual compositions are as rich in wolframite as ~50 and ~70 mol. % (Figs 4c and e, 5c and e, respectively; Tab. 3). In compositional plots, the low but persistent content of Ti in the exsolved phase (Fig. 6) shifts the data points slightly but systematically sideways from the columbite–wolframite join (Fig. 4c, e, 5c, e). The Ta/(Ta + Nb) values of the exsolved ixiolite are largely between 0.05 and 0.08, rarely approaching 0.10, but the Mn/(Mn + Fe) values are very dispersed from 0.01 to 0.35 (Fig. 4d, f, 5 d, f). Individual grains of exsolved ixiolite range from

homogeneous to highly heterogeneous, mainly in terms of tungsten concentration. Figure 1f shows a possibly extreme example of a compositionally heterogeneous grain which varies internally from 3.6 to 38.9 wt. % WO_3; in most other cases, the variation of the W content is more moderate. Relative to the primary and depleted rutile, the exsolved ixiolite is also enriched in Nb, Ta, Fe^{2+}, Mn, Mg, Zr, Hf and Sc, but low in Sn and Fe^{3+} (Tables 1–3, Figs 4, 5, 7e, f).

Overall, the collected data show only minimal differences between the compositions of the phase components of the fine-grained and coarse-grained assemblages. The *relatively* most conspicuous difference is in the degree of exsolution of the main components of the two phases, best shown graphically in Fig. 4c, e and 5c, e. In the coarse-grained material, the rutile phase is slightly more depleted, and the ixiolite phase is slightly lower in Ti and slightly more enriched in W (Tables 2 and 3).

7. Inclusions of an unknown phase

Microscopic inclusions of an unknown phase are extremely rarely found along the contacts of the crystals of niobian rutile with the surrounding albite or tourmaline matrix. They are mostly rounded and intimately intergrown with feldspars and quartz. The identity of these grains cannot be unambiguously established as their size, less than 10 μm, and quasi-skeletal intergrowth with adjacent phases are out of reach of routine XRD methods. Two possibilities may be considered, based on chemical composition alone, but neither seems to be justified: pseudorutile or pseudobrookite (Tab. 4; see "Discussion" below).

8. Discussion

The primary niobian rutile from the Písek pegmatites is distinguished by the ubiquitous oscillatory zoning and high W content. Otherwise, it would represent a typical (Fe, Nb)-dominant phase with $Fe^{2+} >> Fe^{3+}$ and the main substitution of (Fe >> Mn, Mg)$^{2+}_{+1}$ (Nb > Ta)$^{5+}_{+2}$ for Ti^{4+}_{-3}. However, the W^{6+} exerts a substantial influence on the exsolution behavior of the Písek niobian rutile.

8.1. Crystal chemistry of the rutile phase

Figure 8 a–d shows the plots of the primary and depleted rutile compositions on an A^{2+} vs. B^{5+} diagram, compared to the ideal columbite-type 1 : 2 ratio, and the individual data adjusted for other heterovalent substitutions (as homovalent substitutions of Sn, Zr, Hf, U and Th for Ti pose no problem). Excellent agreement of the terms (Fe^{2+}
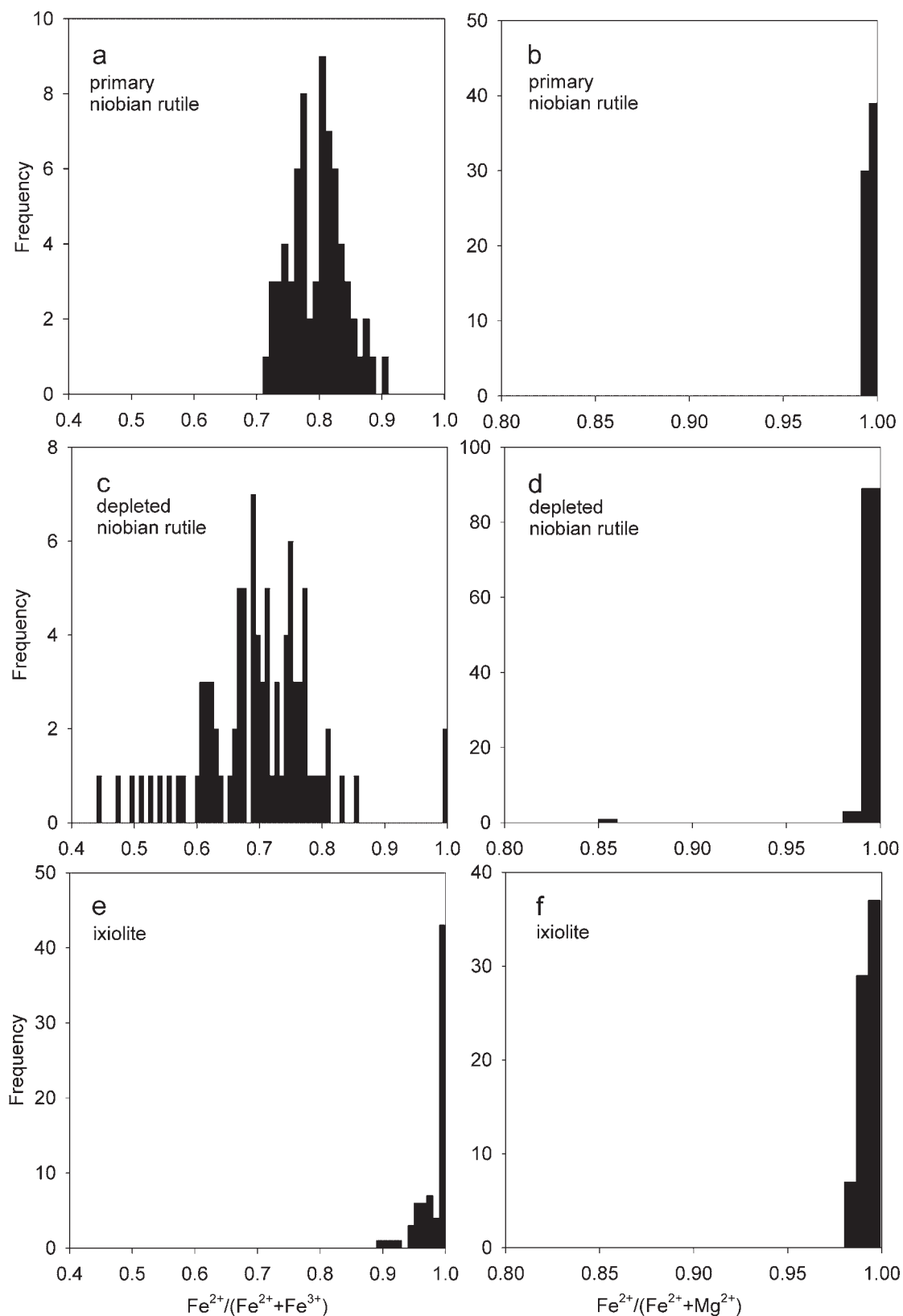
Fig. 7 Histograms of $Fe^{2+}/(Fe^{2+} + Fe^{3+})$ and $Fe^{2+}/(Fe^{2+} + Mg)$ (atomic ratios) in the primary homogeneous niobian rutile (**a–b**), in the depleted fine- and coarse-grained niobian rutile (**c–d**), and in the exsolved fine- and coarse-grained ixiolite (**e–f**); all data in atomic ratios. Exsolution leads to preferential partitioning of Fe^{3+} into the rutile phase, and of Mg into the ixiolite phase.

Tab. 4 Chemical composition of the unknown phase. Samples 46A13 and 46A15 from Údraž, ST314 from Písek. Atomic contents normalized to 5 oxygen atoms and 3 cation atoms of a pseudobrookite-type formula, and to 9 oxygen atoms and 5 cation atoms of a pseudorutile-type formula with all Fe taken as trivalent.

	pseudobrookite			pseudorutile		
Sample	46A13	46A15	ST314	46A13	46A15	ST314
wt. %						
WO_3	0.56	0.60	0.26	0.56	0.60	0.26
Nb_2O_5	2.23	1.81	0.87	2.23	1.81	0.87
Ta_2O_5	0.25	0.14	0.20	0.25	0.14	0.20
TiO_2	58.18	58.18	61.95	58.18	58.18	61.95
ZrO_2	0.00	0.00	0.14	0.00	0.00	0.14
SnO_2	0.03	0.03	0.00	0.03	0.03	0.00
HfO_2	0.00	0.00	0.05	0.00	0.00	0.05
ThO_2	0.00	0.00	0.10	0.00	0.00	0.10
UO_2	0.08	0.08	0.01	0.08	0.08	0.01
Sc_2O_3	0.03	0.07	0.00	0.03	0.07	0.00
Fe_2O_3	4.42	5.90	1.31	30.46	29.32	31.00
Y_2O_3	0.02	0.01	0.00	0.02	0.01	0.00
Sb_2O_3	0.02	0.00	0.00	0.02	0.00	0.00
Bi_2O_3	0.02	0.06	0.03	0.02	0.06	0.03
MgO	0.05	0.10	0.02	0.05	0.10	0.02
CaO	0.06	0.05	0.04	0.06	0.05	0.04
MnO	3.44	4.96	1.57	3.44	4.96	1.57
FeO	23.44	21.08	26.72	—	—	—
ZnO	0.02	0.10	0.00	0.02	0.10	0.00
PbO	0.06	0.15	0.19	0.06	0.15	0.19
Total	92.91	93.32	93.46	95.51	95.66	96.43
W^{6+}	0.006	0.007	0.003	0.010	0.011	0.005
Nb^{5+}	0.043	0.034	0.016	0.071	0.057	0.027
Ta^{5+}	0.003	0.002	0.002	0.005	0.003	0.004
Ti^{4+}	1.847	1.837	1.941	3.079	3.061	3.235
Zr^{4+}	0.000	0.000	0.003	0.000	0.000	0.005
Sn^{4+}	0.001	0.001	0.000	0.001	0.001	0.000
Hf^{4+}	0.000	0.000	0.001	0.000	0.000	0.001
Th^{4+}	0.000	0.000	0.001	0.000	0.000	0.002
U^{4+}	0.001	0.001	0.000	0.001	0.001	0.000
Sc^{3+}	0.001	0.003	0.000	0.002	0.004	0.000
Fe^{3+}	0.140	0.186	0.041	1.613	1.544	1.620
Y^{3+}	0.000	0.000	0.000	0.001	0.000	0.000
Sb^{3+}	0.000	0.000	0.000	0.001	0.000	0.000
Bi^{3+}	0.000	0.001	0.000	0.000	0.001	0.001
Mg^{2+}	0.003	0.006	0.001	0.005	0.010	0.002
Ca^{2+}	0.003	0.002	0.002	0.005	0.004	0.003
Mn^{2+}	0.123	0.176	0.055	0.205	0.294	0.092
Fe^{2+}	0.827	0.740	0.931	—	—	—
Zn^{2+}	0.001	0.003	0.000	0.001	0.005	0.000
Pb^{2+}	0.001	0.002	0.002	0.001	0.003	0.004

+ Mn + Mg – W) and (Nb + Ta – Fe^{3+}– Sc) confirms both the principal mechanism of incorporation of the divalent and pentavalent cations $A^{2+}B^{5+}_2 Ti^{4+}_{-3}$, and the substitutions $(Fe > Sc)^{3+}_{+1} (Nb > Ta)^{5+}_{+1} Ti^{4+}_{-2}$ plus $(Fe >> Mn, Mg)^{2+}_{+1}$

$W^{6+}_{+1} Ti^{4+}_{-2}$, incorporated into the terms quoted above. This virtually ideal compliance with the proposed substitutions is probably slightly exaggerated by an assumption of full cation occupancy in both rutile phases and calculation of the $Fe^{2+}$and Fe^{3+}contents, but it should be at least very close to reality. In any case, the diagrams confirm the absence of any significant substitutions other than the three quoted above.

8.2. Oscillatory zoning in the primary niobian rutile

The virtually omnipresent oscillatory zoning in the niobian rutile from both localities examined, never observed in other pegmatite-hosted occurrences of this mineral, poses a problem. Fluctuations of activity of the components involved in the parent medium are a possibility. However, the fluctuations would have to be synchronized among at least four cations (Fe^{2+}, Mn^{2+}, Nb^{5+} and Ta^{5+}). Differences in diffusion rates of diverse cations at the boundary layer of the parent medium along the growth surfaces of niobian rutile can be expected. The details of the Nb + Ta oscillation pattern are in apparent agreement with this mechanism (Fig. 3; gradual increase and saturation of heavy species followed by their sudden depletion; Butler and Thompson 1965; Černý et al. 1985). However, the largely independent (up to erratic) behavior of W does not fit this concept: W is about equal in atomic mass to Ta, and it should show about the same difference in diffusion from Ti (see Carruzzo et al. 2006 for more detailed discussion of zoning in rutile and Bryksina et al. 2006 for a general account of oscillatory zoning).

The lack of a distinctive oscillatory and/or sectorial zoning of the W content is in sharp contrast with prominent display of these features by tungstenian rutile from a hydrothermal milieu, which did not induce exsolution (Smith and Perseil 1997; Rice et al. 1998). It should be noted, however, that in these cases the substitution schemes introducing W into the rutile structure are different from that observed here.

8.3. Crystal chemistry of the ixiolite phase

As discussed earlier, XRD powder data and the chemical compositions do not provide an unambiguous identity of the exsolved phase, and the designation of (titanian–tungstenian) ixiolite is, to a degree, provisional. Compared to the data of Černý et al. (1998), the relatively low content of Ti would probably qualify this phase for titanian ferrocolumbite, which converts to an ordered columbite structure on heating. However, the presence of modest up to very substantial W complicates the matter. There is a plethora of "wolframo-ixiolites" described in the literature (Amichba and Dubakina 1974; Borneman-
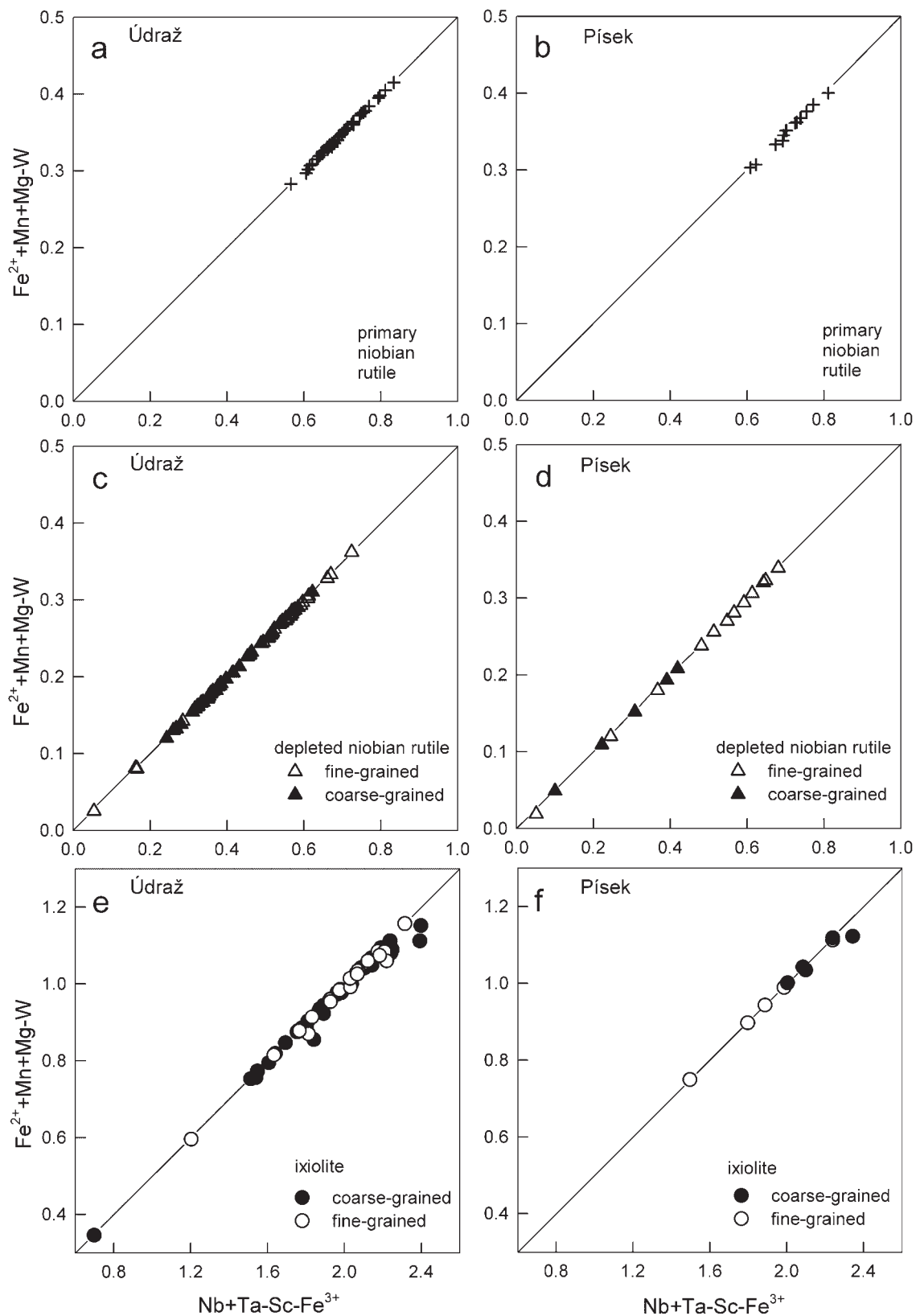
Fig. 8 Correlation of the terms (Fe^{2+} + Mn + Mg - W) and (Nb + Ta - Sc - Fe^{3+}) (atomic values) in primary niobian rutile, depleted niobian rutile and ixiolite.

Starynkevitch et al. 1974; Konovalenko et al. 1982; Yang et al. 1985 [qitianlingite]; Kluger and Pertlik 1985; Wang et al. 1988), more or less defined chemically and structurally, and it is questionable whether the exsolved phase could be identical with any of them, even were sufficient quantities of homogeneous material available for a more complete characterization. Moreover, the composition most enriched in W (Tab. 3, # N34A1) is very close to that of niobian wolframite from Mozambique (Saari et al. 1968) and niobian ferberite from Dolní Bory (Novák and Šrein 1989; Novák et al. 2007). In view of the very extensive miscibility gap in the $FeWO_4$–$FeNb_2O_6$ system at temperatures realistic for crystallization of granitic pegmatites (Schröcke 1961), and of the locally remarkable heterogeneity of the exsolved phase (Fig. 1f), it is probable that the exsolution generated metastable disequilibrium products, some of which broke down on continued cooling, and its components may now belong to two or more structural types.

In any case, Fig. 8e–f shows that the same terms can describe the substitution mechanisms in the ixiolite as those used for the rutile phases. Here, however, these terms cover the locally dominant heterovalent scheme $(Fe^{2+}_3W^{6+}_3)_{+1}(Fe^{2+}_2Nb^{5+}_4)_{-1}$, which can be condensed to $Fe^{2+}_{+1}W^{6+}_{+3}Nb^{5+}_{-4}$; the much less expressed $(Fe > Sc)^{3+}_{+3}$ $(Fe \gg Mn, Mg, Ca)^{2+}_{-2} (Nb > Ta)^{5+}_{-1}$; and the reversal of the main mechanism operating in the niobian rutile: subordinate but steady $(Ti \gg Zr, Hf)^{4+}_{+3} (Fe \gg Mn, Mg, Ca)^{2+}_{-1} (Nb > Ta)^{5+}_{-2}$, which, however, does not affect the reference ratio $(Fe, Mn, Mg, Ca)^{2+}/(Nb, Ta)^{5+}$ of 0.5. The correlation shown in Fig. 8e–f is imperfect, in part probably due to minor quantities of Y, Bi, Sb, As and Pb. Substitution mechanisms additional to those quoted here may be involved, utilizing some of the Ti, Sc and Fe^{3+} outside the schemes shown above (e.g., Johan and Johan 1994), and they may account for some of the deviations from the 0.5 line; however, they are out of reach of reliable quantitative confirmation.

8.4. What is the identity of the unknown phase?

As indicated in the descriptive part above, the chemical composition of this phase seems to best correspond to that of pseudobrookite or pseudorutile. However, problems arise with either of these interpretations.
Normalization to 5 oxygen atoms and 3 cations, involving calculation of ferric iron (Tab. 4), yields atomic contents very close to the formula of "ferropseudobrookite" $Fe^{2+}Ti^{4+}_2O_5$, with a limited proportion of the armalcolite-type component $(Mn \gg Ca, Mg)^{2+}Ti^{4+}_2O_5$ and a similarly minor presence of the "ferripseudobrookite" end member $Fe^{3+}_2Ti^{4+}O_5$ (Bowles 1988; cf. Uher et al. 1998). However, the wt. % total is ~7 % short of 100 for all analyzed spots,

in disagreement with the anhydrous constitution of the pseudobrookite-group minerals, and no components other than those quoted in Tab. 4 could be detected.

Recalculation in the pseudorutile style, with all Fe as ferric, also yields unacceptable results. Low wt. % totals are common in pseudorutile, which tends to be in most cases slightly hydrated (either in its primary state, or by incipient alteration of pristine $Fe^{3+}_2Ti_3O_9$; Grey and Reid 1975; Grey et al. 1994), but the stoichiometry of our mineral shows deficit in Fe^{3+} (even if its site occupancy is boosted by Mn^{2+}), and an excess of Ti (Tab. 4).

8.5. Miscellaneous crystal-chemical and geochemical correlations

Behavior of Ti. Titanium content of the primary homogeneous niobian rutile is restricted to a narrow range, with a near-Gaussian distribution (Fig. 6a). In contrast, Ti in the depleted niobian rutile is much more variable, reflecting the different degrees of unmixing of the ixiolite component (Fig. 6a). The exsolved ixiolite shows again a very narrow range of the Ti content (Fig. 6b). Figures 5c, e and 6c, e are somewhat misleading in this respect, as the spread of ixiolite plots into the field of the diagram reflects not only the Ti content but also is strongly influenced by W.

Distribution of Fe^{2+}, Fe^{3+} and Mg. Only a small proportion of Fe in the primary homogeneous niobian rutile is trivalent (Fig. 7a). The average value of $Fe^{2+}/(Fe^{2+} + Fe^{3+})$ in this phase is 0.80, somewhat lower than 0.85 found for the primary homogeneous niobian rutile from Věžná (Černý et al. 2000b). On exsolution, Fe^{3+} is preferably retained in the depleted rutile, whereas ixiolite is dominated by Fe^{2+} (Fig. 7c, e). On the contrary, Mg shows a definite preference for the ixiolite structure (Fig. 7b, d, f). The close similarity of the ionic radii of Mg^{2+} and Fe^{2+}, tailored to the columbite structure, compared to the smaller but mutually comparable radii of Fe^{3+} and Ti, explain this distribution of the ferran and ferrian iron.

The generally low Mg content supports the contention of Černý et al. (2000b), that the rather high Mg in the Věžná niobian rutile and exsolved ferrocolumbite comes from contamination of the pegmatite magma by reaction with its ultrabasic host rock. The Věžná pegmatite (which also carries beryllian cordierite and Mg-enriched tourmaline) intruded a serpentinite body, whereas the Údraž and Písek pegmatites reside in biotite gneiss, locally migmatite, and partly also in melasyenite (Písek).

Scandium and ferric iron. In contrast to the above, the Sc^{3+} and Fe^{3+} contents of the exsolved ixiolite do not show any mutual affinity (Fig. 9b). This is contrary to expectation, as these two cations commonly show a close relationship in numerous other geological environments (e.g., Wise et al. 1998; Novák and Černý 1998), but this
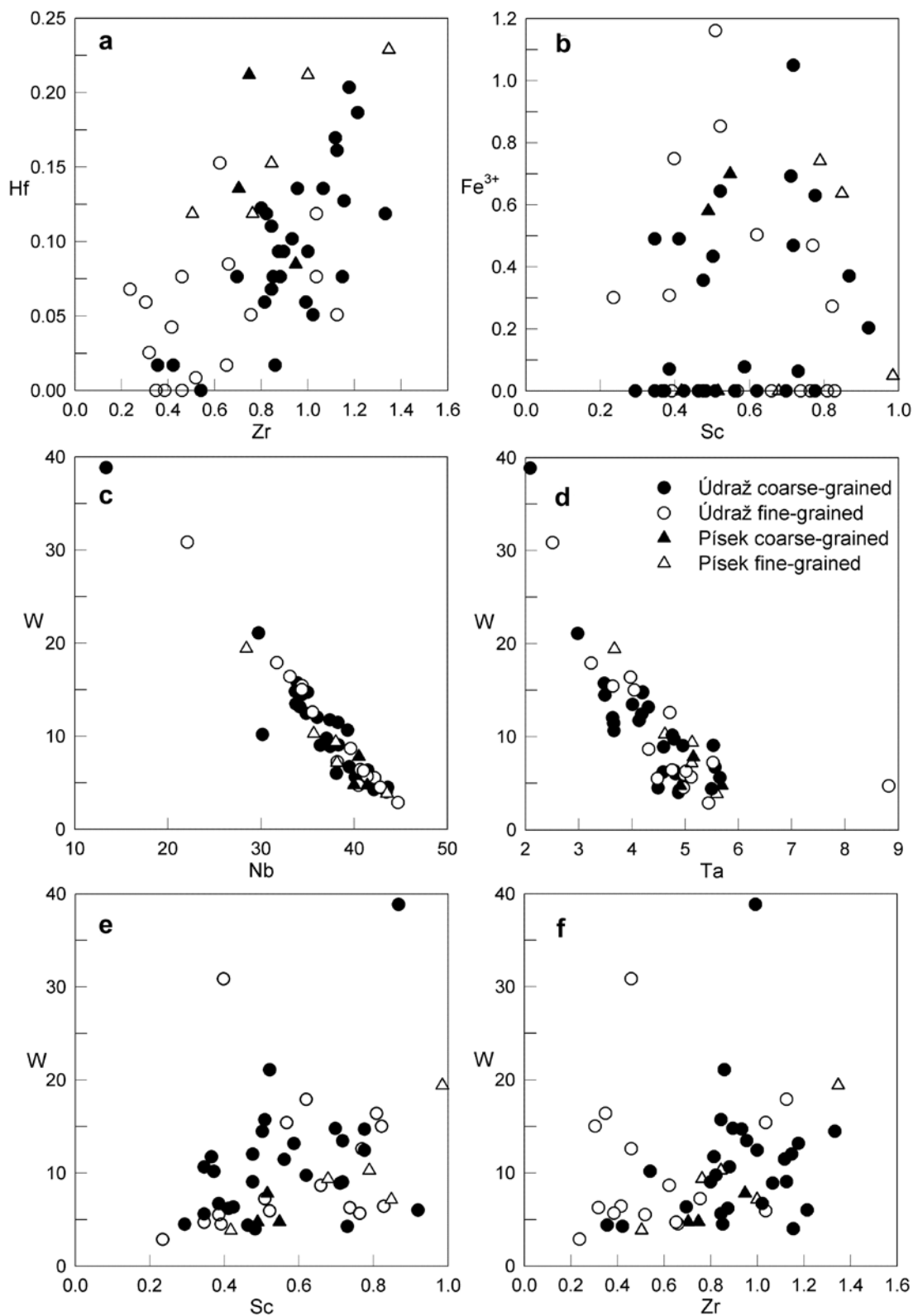
Fig. 9 Miscellaneous correlations in the exsolved tungstenian–titanian ixiolite (wt. %): **a** – poorly defined positive trend of Zr and Hf, undoubtedly affected by the low Hf concentrations, close to the detection limit; **b** – general lack of correlation between Sc and Fe^{3+}; **c** and **d** – negative trends of W versus Nb and Ta, respectively (note the difference in scales between Nb and Ta); **e** and **f** – poor positive correlation of W with Sc and Zr, respectively.

lack of correlation matches that found in the ferrocolumbite exsolutions from Věžná (Černý et al. 2000b).

Zirconium and hafnium. Figure 9a shows a poorly expressed, nevertheless noticeable positive correlation of Zr and Hf in the ixiolite, similar to that observed in ferrocolumbite exsolved from the Věžná niobian rutile (Černý et al. 2000b), and in wodginite exsolved from the Annie Claim #3 cassiterite (Masau et al. 2000). The poor correlation is in part undoubtedly caused by the high analytical error in determination of Hf, as most of its values are close to the detection limit (see Černý et al. 2007). Nevertheless, the data confirm the conclusion of Černý et al. (2000b) that limited quantities of Zr and Hf do enter the structure of niobian rutile, and are preferentially extracted into the orthorhombic phase on exsolution. The main cluster of data for ixiolite exsolutions in Fig. 9a corresponds to Zr/Hf values in the 16 to 5 range, which is in good agreement with that found in the associated zircon, 14.8 to 4.8.

Tungsten. The mode of incorporation of W, discussed earlier, and Figs 4 and 5 imply a negative correlation between W on one side and Nb and Ta on the other. Figure 9c–d shows this relationship to be close to linear, taking into account the difference in the Nb and Ta scales. The modest lateral scatter across the trends is caused by the steady but somewhat variable content of Ti, and of other rather minor quadrivalent cations. There seems to be a degree of positive correlation between W and Sc, and between W and Zr (Fig. 9e, f, respectively). Neither of them is, however, well defined; the best that can be said is that with increasing W, the number of data with high Sc and Zr also increases, but they do not surpass the highest values found in the W-poor compositions.

Elemental distribution between exsolved phases. Exsolution of the ixiolite phase tends to eliminate most of the major and minor constituents from the rutile structure, whereas the ixiolite is rather poor in Ti. In relative terms, rutile retains Ta, Fe^{2+} and Fe^{3+}, and Fe^{3+} relative to Fe^{2+}, and the ixiolite attracts mainly Mn and Nb. Preferred removal of Nb, Mn, Mg, Zr, Hf and Sc from rutile, but a degree of retention of Ta, Fe^{2+}, Fe^{3+} and Sn in this phase is in agreement with the structural preferences of their Ti-free compounds. Cassiterite and ferrotapiolite $Fe^{2+}Ta_2O_6$ are isostructural with rutile, tantalian rutile generally remains stable on cooling (Černý et al. 1964), and Fe^{3+} is very close to the r_i of Ti^{4+}, whereas $MnTa_2O_6$ and Mg- and Nb-dominant members of the columbite group are orthorhombic. The relatively large ionic radii of Zr^{4+}, Hf^{4+} and Sc^{3+} exceed that of Ti^{4+} by more than 20 %, which renders them more compatible with the structure of columbite and related (Nb, Ta)-oxide minerals (Černý et al. 2007).

Correlation of composition, grain size and exsolution style. In contrast to the Věžná niobian rutile, in which the degree of exsolution remarkably increases with grain size of the exsolution products, such a trend is hardly noticeable in the south-Bohemian samples (Figs 4, 5, 8, 9) that also are relatively more uniform in grain size. A rather fast, single-step exsolution is suspected here, whereas a gradual three-step process was considered possible at Věžná (Černý et al. 2000b). A rapid single-step exsolution would also be compatible with the broad compositional range of the exsolved phases, and with the possibility of later breakdown of early exsolution products (Fig. 1f).

9. Conclusions

Our results confirm the capacity of niobian rutile from a pegmatitic environment to incorporate modest quantities of W^{6+}, *via* the substitution $(Fe, Mn, Mg)^{2+}_{+1} W^{6+}_{+1} Ti^{4+}_{-2}$. Oscillatory compositional zoning of the primary rutile is, however, restricted to the columbite-type substitution of Nb and Ta component, whereas the behavior of W is rather random. This is in sharp contrast to retention of W in rutile, and its locally zonal plus sectorial distribution, in hydrothermal assemblages, which involves different valence-compensating mechanisms. Most of the Nb, Ta, W and Fe, plus a host of minor elements, are exsolved from the south-Bohemian niobian rutile in the form of an orthorhombic columbite-like phase on cooling. Disordered ixiolite-type state is suspected, but more than a single mineral may be involved, in view of the complex chemical composition and highly variable W content of different grains and subgrains. The W substitution $Fe^{2+}_{+1} W^{6+}_{+3} Nb^{5+}_{-4}$ broadens the spectrum of four other modifications of rutile chemistry in granitic pegmatites, involving Nb, Ta and various proportions of divalent and trivalent cations that trigger diverse types of exsolution.

References

AMICHBA TM, DUBAKINA LS (1974) Wolframoixiolite in ores of tungsten deposits of Yakutia. Sborn Nauchn Trud Mosk Otdel Vses Mineral Obshch 1974: 11–18 (in Russian)

Borneman-Starynkevitch ID, Rudnitskaya ES, Loseva TI, Amelina VS (1974) Once again, wolframoixiolite. Sborn Nauchn Trud Mosk Otdel Vses Mineral Obshch 1974: 25–28 (in Russian)

Bowles JFW (1988) Definition and range of composition of naturally occurring minerals with the pseudobrookite structure. Amer Miner 73: 1377–1383

Bryksina NA, Halden NM, Mejia S (2006) Qualitative and quantitative characteristics of modelled and natural oscillatory zoning patterns in calcite. Math Geol 38: 635–655

Butler JR, Thompson AJ (1965) Zirconium:hafnium ratio in some igneous rocks. Geochim Cosmochim Acta 16: 151–180

Carruzzo S, Clarke DB, Pelrine KM, MacDonald MA (2006) Texture, composition, and origin of rutile in the South Mountain batholith, Nova Scotia. Canad Mineral 44: 715–729

Čech F, Černý P, Povondra P (1964) Ilmenorutile from Údraž near Písek and products of its breakdown. Acta Univ Carol, Geol 1: 1–14 (in Czech)

Čech F, Staněk J, Dávidová Š (1981) Pegmatite minerals. In: Bernard JH (ed) Mineralogy of Czechoslovakia – 2nd ed. Academia, Praha, 98–183 (in Czech)

Černý P, Chapman R (2001) Exsolution and breakdown of scandian and tungstenian Nb–Ta–Ti–Fe–Mn phases in niobian rutile. Canad Mineral 39: 93–101

Černý P, Ercit TS (2005) The classification of granitic pegmatites revisited. Canad Mineral 43: 2005–2026

Černý P, Čech F, Povondra P (1964) Review of ilmenorutile–strüverite minerals. Neu Jb Mineral, Abh 101: 142–172

Černý P, Meintzer RE, Anderson AJ (1985) Extreme fractionation in rare-element granitic pegmatites: selected examples of data and mechanisms. Canad Mineral 23: 381–421

Černý P, Ercit TS, Wise MA, Buck HM (1998) Compositional, structural and phase relationships in titanian ixiolite and titanian columbite–tantalite. Canad Mineral 36: 547–562

Černý P, Chapman R, Simmons WB, Chackowsky LE (1999) Niobian rutile from the McGuire granitic pegmatite, Park County, Colorado: solid solution, exsolution, and oxidation. Amer Miner 84: 754–763

Černý P, Chapman R, Masau M (2000a) Two-stage exsolution of a titanian (Sc, Fe^{3+})(Nb, Ta)O$_4$ phase in Norwegian niobian rutile. Canad Mineral 38: 907–913

Černý P, Novák M, Chapman R, Masau M (2000b) Subsolidus behavior of niobian rutile from Věžná, Czech Republic: a model for exsolution in phases with Fe^{2+} >> Fe^{3+}. J Czech Geol Soc 45: 21–35

Černý P, Ercit TS, Smeds S-A, Groat LA, Chapman R (2007) Zirconium and hafnium in minerals of the columbite and wodginite groups from granitic pegmatites. Canad Mineral (in press)

Ercit TS, Černý P, Hawthorne FC, McCammon CA (1992) The wodginite group. II. Crystal chemistry. Canad Mineral 30: 613–631

Graham J, Morris RC (1973) Tungsten- and antimony-substituted rutile. Mineral Mag 39: 470–473

Grey IE, Reid AF (1975) The structure of pseudorutile and its role in the natural alteration of ilmenite. Amer Mineral 60: 898–906

Grey IE, Watts JA, Bayliss P (1994) Mineralogical nomenclature: pseudorutile revalidated and neotype given. Mineral Mag 58: 597–600

Johan V, Johan Z (1994) Accessory minerals of the Cínovec (Zinnwald) granite cupola, Czech Republic Part 1: Nb-, Ta- and Ti-bearing oxides. Mineral Petrol 51: 323–343

Kluger F, Pertlik F (1985) Wolframoixiolite from Isola d'Elba, Italy. Abstracts, vol. 1, 9th Eur. Crystallogr. Meeting Torino, pp 454

Konovalenko SI, Voloshin AV, Pakhomovskyi YaA, Rossovskyi LN, Ananiev SA (1982) Tungsten-bearing varieties of tantaloniobates from miarolitic granite pegmatites of southwestern Pamir. Mineral Zhurnal 4: 65–74 (in Russian)

Kovář F (1895) Analyses of some minerals, particularly from the Písek region. Listy chemické 19: 62–65

Masau M, Černý P, Chapman R (2000) Exsolution of zirconian-hafnian wodginite from manganoan–tantalian cassiterite, Annie Claim #3 granitic pegmatite, southeastern Manitoba, Canada. Canad Mineral 38: 685–694

Nováček R (1936) Several notes on the mineralogy of the Písek region. Vědy přírodní 17: 228–230 (in Czech)

Novák M (2005) Granitic pegmatites of the Bohemian Massif (Czech Republic); mineralogical, geochemical and regional classification and geological significance. Acta Mus Moraviae Sci Geol 90: 3–74 (in Czech)

Novák M, Černý P (1998) Scandium in columbite-group minerals from LCT pegmatites in the Moldanubicum, Czech Republic. Krystalinikum 24: 73–89

Novák M, Šrein V (1989) Chemical composition and paragenesis of wolframite from the Dolní Bory pegmatites, western Moravia, Czechoslovakia. Acta Univ Carol, Geol Čech Vol: 495–500

Novák M, Johan Z, Škoda R, Černý P (2007) Complex W, Nb, U, Ti, Fe-oxide minerals from the granitic pegmatite No. 3, Dolní Bory – Hatě, Czech Republic. In: Martins T, Vieira R (eds) Granitic Pegmatites: The State of Art, Porto May 2007, Book of Abstracts, pp 68–69

Okrusch M, Hock R, Schüssler U, Brummer A, Baier M, Theisinger H (2003) Intergrown niobian rutile phases with Sc- and W-rich ferrocolumbite: An electron-microprobe and Rietveld study. Amer Miner 88: 986–995

Pouchou JL, Pichoir F (1984) A new model for quantitative analysis. I. Application to the analysis of homogeneous samples. La Récherche Aerosp 3: 13–38

Pouchou JL, Pichoir F (1985) "PAP" Φ (ρZ) procedure for improved quantitative microanalysis. – In: Armstrong, JT (ed): Microbeam Anal. 1985, San Francisco Press, San Francisco, California: 104–106

Rice CM, Darke KE, Still JW (1998) Tungsten-bearing rutile from the Kori Kollo gold mine, Bolivia. Mineral Mag 62: 421–429

Saari E, Knorring Ov, Sahama ThG (1968) Niobian wolframite from the Nuaparra pegmatite, Zambezia, Mozambique. Lithos 1: 164–168

Sahama ThG (1978) Niobian rutile from Muiane, Mozambique. Jornal de Mineralogia Recife, vol. Djalma Guimarẽs 7: 115–118

Schröcke H (1961) Heterotype Mischbarkeit zwischen Wolframit- und Columbitgruppe. Beitr Mineral Petrogr 8: 92–108

Smith DC, Perseil EA (1997) Sb-rich rutile in the manganese concentrations at St. Marcel-Praborna, Aosta Valley, Italy: petrology and crystal chemistry. Mineral Mag 61: 655–669

Uher P, Černý P, Chapman R, Határ J, Miko O (1998) Evolution of Nb, Ta-oxide minerals in the Prašivá granitic pegmatites, Slovakia. I. Primary Fe, Ti-rich assemblage. Canad Mineral 36: 525–534

Urban AJ, Hoskins BF, Grey IE (1992) Characterization of V–Sb–W-bearing rutile from the Hemlo gold deposit, Ontario. Canad Mineral 30: 319–226

Voloshin AV, Gordiyenko VV, Pakhomovskyi YaA (1991) On scandian mineralization and the first find of thortveitite in granitic pegmatites of the Kola Peninsula. Dokl Akad Nauk USSR 318: 972–976 (in Russian)

Vrba K (1893) On Czech minerals. Listy chemické 17: 64–66 (in Czech)

Wang S, Ma Z, Peng Z (1988) The crystal structure of wolframoixiolite. Kexue Tongbao (Foreign Language Edition) 33: 1363–1366

Wise MA, Černý P, Falster AU (1998) Scandium substitution in columbite-group minerals and ixiolite. Canad Mineral 36: 673–680

Yang G, Wang S, Peng Z, Bu J (1985) Qitianlingite – a newly discovered superstructure complex oxide. Acta Mineral Sinica 5: 193–198 (in Chinese)

Chování niobového rutilu z Písecka v České Republice v subsolidu: model pro odmíšení fází bohatých na W a Fe²⁺

Niobový rutil s podstatným obsahem W se vyskytuje společně s černým turmalínem, berylem, zirkonem, xenotimem-(Y), monazitem-(Ce), "písekitem" a neznámým minerálem Fe a Ti ve dvou kogenetických granitických pegmatitech beryl-columbitového subtypu u Písku a Údraže v jižních Čechách. Krystaly, až 3 × 1 cm velké, uzavírají relikty primárního, oscilačně zonárního niobového rutilu v agregátech niobem ochuzeného rutilu uzavírajícího hojné odmíšeniny titanem a wolframem obohaceného ixiolitu. Primární niobový rutil má monorutilovou strukturu a podstatnou substituci (Fe > Mn, Mg)$^{2+}_{+1}$ (Nb > Ta)$^{5+}_{+2}$ Ti$^{4+}_{-3}$ (až 26.34 hm. % Nb$_2$O$_5$ a 8.60 hm.% Ta$_2$O$_5$; 26 až 37 mol. % columbitové komponenty), výrazné zastoupení (Fe >> Mn, Mg)$^{2+}_{+1}$ W$^{6+}_{+1}$ Ti$^{4+}_{-2}$ (až 3.12 hm.% WO$_3$) a podřadný podíl (Fe > Sc)$^{3+}_{+1}$ (Nb > Ta)$^{5+}_{+1}$ Ti$^{4+}_{-2}$. Hodnoty Fe^{2+}/(Fe^{2+}+ Fe^{3+}) jsou vysoké, v průměru ~ 0.8. Oscilační zonálnost je kontrolována niobem, tantalem a železem, kolísání wolframu je na nich nezávislé a nahodilé. Ochuzený niobový rutil stále ještě obsahuje 8 až (zřídka) 32 mol. % columbitové komponenty. Jednotlivá zrna odmíšeného ixiolitu jsou často heterogenní se silně kolísajícím obsahem W, vstupujícím substitucí Fe$^{2+}_{+1}$W$^{6+}_{+3}$Nb$^{5+}_{-4}$ (až 49.00 hm. % WO$_3$). Zastupování (Ti >> Zr, Hf)$^{4+}_{+3}$ (Fe >> Mn, Mg, Ca)$^{2+}_{-1}$ (Nb > Ta)$^{5+}_{-2}$ (až 9.83 hm. % TiO$_2$, 1.94 hm. % ZrO$_2$), a (Fe > Sc)$^{3+}_{+3}$ (Fe >> Mn, Mg, Ca)$^{2+}_{-2}$ (Nb > Ta)$^{5+}_{-1}$ (až 1.51 hm. % Sc$_2$O$_3$) jsou podřadná. Odmíšení ukazuje preferenci Sn a Fe^{3+} pro rutilovou strukturu, zatímco Fe^{2+}, Mn, Mg, Nb, Ta, Sc, Zr, Hf a W jsou koncentrovány v ixiolitu. Výsledky potvrzují možnost rozsáhlé substituce wolframitové komponenty v niobovém rutilu z granitických pegmatitů a její význam pro styl odmíšení, srovnatelný se stupněm vlivu kombinaci Nb > Ta + Fe^{2+}, Nb > Ta + Sc + Fe^{3+}, Nb > Ta + (Fe^{2+}/Fe^{3+}~1), nebo Fe/(Nb > Ta) > 0.5.